



Comprehensive Transcriptome Profiling of Cryptic *CBFA2T3-GLIS2* Fusion-Positive AML Defines Novel Therapeutic Options: A COG and TARGET Pediatric AML Study

Jenny L. Smith¹, Rhonda E. Ries¹, Tiffany Hylkema¹, Todd A. Alonzo^{2,3,4}, Robert B. Gerbing², Marianne T. Santaguida⁵, Lisa Eidenschink Brodersen⁶, Laura Pardo^{1,6}, Carrie L. Cummings¹, Keith R. Loeb¹, Quy Le¹, Suzan Imren¹, Amanda R. Leonti¹, Alan S. Gamis⁷, Richard Aplenc⁸, E. Anders Kolb⁹, Jason E. Farrar¹⁰, Timothy J. Triche Jr¹¹, Cu Nguyen¹², Daoud Meerzaman¹², Michael R. Loken⁶, Vivian G. Oehler¹, Hamid Bolouri¹³, and Soheil Meshinchi^{1,2,14}

ABSTRACT

Purpose: A cryptic *inv(16)(p13.3q24.3)* encoding the *CBFA2T3-GLIS2* fusion is associated with poor outcome in infants with acute megakaryocytic leukemia. We aimed to broaden our understanding of the pathogenesis of this fusion through transcriptome profiling.

Experimental Design: Available RNA from children and young adults with *de novo* acute myeloid leukemia (AML; *N* = 1,049) underwent transcriptome sequencing (mRNA and miRNA). Transcriptome profiles for those with the *CBFA2T3-GLIS2* fusion (*N* = 24) and without (*N* = 1,025) were contrasted to define fusion-specific miRNAs, genes, and pathways. Clinical annotations defined distinct fusion-associated disease characteristics and outcomes.

Results: The *CBFA2T3-GLIS2* fusion was restricted to infants <3 years old (*P* < 0.001), and the presence of this fusion was highly associated with adverse outcome (*P* < 0.001) across all morphologic classifications. Further, there was a striking paucity of recurrent cooperating mutations, and transduction of cord blood

stem cells with this fusion was sufficient for malignant transformation. *CBFA2T3-GLIS2* positive cases displayed marked upregulation of genes with cell membrane/extracellular matrix localization potential, including *NCAM1* and *GABRE*. Additionally, miRNA profiling revealed significant overexpression of mature *miR-224* and *miR-452*, which are intronic miRNAs transcribed from the *GABRE* locus. Gene-set enrichment identified dysregulated Hippo, TGFβ, and hedgehog signaling, as well as *NCAM1* (CD56) interaction pathways. Therapeutic targeting of fusion-positive leukemic cells with CD56-directed antibody-drug conjugate caused significant cytotoxicity in leukemic blasts.

Conclusions: The *CBFA2T3-GLIS2* fusion defines a highly refractory entity limited to infants that appears to be sufficient for malignant transformation. Transcriptome profiling elucidated several highly targetable genes and pathways, including the identification of CD56, providing a highly plausible target for therapeutic intervention.

Introduction

Pediatric acute myeloid leukemia (AML) is characterized by significant cytogenetic and molecular heterogeneity. However, the number of patients with AML having clinically actionable variants is limited (1). Although the majority of patients have identifiable chromosomal abnormalities, up to 20% of children have no cytogenetic abnormalities (1, 2). Genomic profiling of megakaryocytic AML (French-American-British classification M7) identified a cryptic *CBFA2T3-GLIS2* fusion that was associated with adverse outcome (3, 4). Although *CBFA2T3-GLIS2* was subsequently found to be enriched in children with normal cytogenetics (CN-AML), and later, not exclusive to either CN or M7 AML (3, 5–7), the prevalence and prognostic significance of *CBFA2T3-GLIS2* in a large heterogeneous cohort of patients have not been fully evaluated.

CBFA2T3 was initially identified as a fusion partner with *RUNX1* in therapy-related AML and shown to facilitate transcriptional repression, as well as being implicated in hematopoietic stem cell quiescence (3). *GLIS2* is closely related to the GLI subfamily and likely functions in modulating the hedgehog signaling pathway (8, 9). The fusion of *GLIS2* to *CBFA2T3* as a result of *inv(16)(p13.3q24.3)* leads to increased expression of the *GLIS2* DNA-binding domain (3). A number of important features of *CBFA2T3-GLIS2* AML have been identified through

¹Clinical Research Division, Fred Hutchinson Cancer Research Center, Seattle, Washington. ²Children's Oncology Group, Monrovia, California. ³Division of Biostatistics, University of Southern California, Los Angeles, California. ⁴Children's Oncology Group, Department of Preventive Medicine, University of Southern California, Monrovia, California. ⁵Notable Laboratories, San Francisco, California. ⁶Hematologics Inc, Seattle, Washington. ⁷Children's Mercy Cancer Center, Kansas City, Missouri. ⁸Department of Pediatrics, Children's Hospital of Philadelphia, Philadelphia, Pennsylvania. ⁹Nemours Alfred I. duPont Hospital for Children, Wilmington, Delaware. ¹⁰UAMS, Arkansas Children's Hospital, Little Rock, Arkansas. ¹¹Van Andel Research Institute, Grand Rapids, Michigan. ¹²Center for Biomedical Informatics and Information Technology, NCI, Rockville, Maryland. ¹³Informatics and Computational Biology, Allen Institute, Seattle, Washington. ¹⁴Department of Pediatrics, University of Washington, Seattle, Washington.

Note: Supplementary data for this article are available at Clinical Cancer Research Online (<http://clincancerres.aacrjournals.org/>).

Corresponding Authors: Jenny L. Smith, Fred Hutchinson Cancer Research Center, 1100 Fairview Avenue North, Seattle, WA 98109. Phone: 206-667-4113; E-mail: jlsmith3@fredhutch.org; and Soheil Meshinchi, Phone: 206-667-4077; Fax: 206-667-4310; E-mail: smeshinc@fhcrc.org

Clin Cancer Res 2020;26:726–37

doi: 10.1158/1078-0432.CCR-19-1800

©2019 American Association for Cancer Research.

Translational Relevance

The *CBFA2T3–GLIS2* fusion is a potent fusion oncogene that leads to a highly refractory phenotype in pediatric acute myeloid leukemia (AML). Transcriptome profiling of 1,049 pediatric AML patients defined a unique expression profile for this fusion and identified a number of altered pathways and potential therapeutic targets, including NCAM1 (CD56). We further demonstrated that the *CBFA2T3–GLIS2* fusion is sufficient for malignant transformation, causally associated with expression of CD56, and its induction in cord blood stem cells recapitulates human disease. The causal association between the fusion oncogene and surface CD56 expression, as well as the promising results of the CD56-ADC (antibody–drug conjugate) across four independent primary samples, provides a viable target that may be curative for these highly refractory patients. Although at present targeted therapies are not clinically available, the vast body of data generated defines fusion oncoprotein–mediated alterations that can be used for the development of precisely directed targeted therapies.

molecular experiments and next-generation sequencing analyses. Acute megakaryoblastic leukemia (AMKL) with *CBFA2T3–GLIS2* displayed altered expression and activation of hedgehog and bone morphogenic signaling pathways, thereby representing potential therapeutic targets (3, 10, 11). Further genomic interrogation of fusion-positive AMKL cell lines identified overexpression of *ERG* transcripts and a synergistic relationship between the *CBFA2T3–GLIS2* oncoprotein and the transcription factor *ERG*, which primes the leukemic phenotype and blocks differentiation (12). In addition, *CBFA2T3–GLIS2* positive cases were found to overexpress the cell-surface marker CD56 (*NCAM1*), and chromatin immunoprecipitation demonstrated that the fusion protein binds to the proximal promoter, inducing its overexpression (4, 13).

However, previous genomic and transcriptomic studies of *CBFA2T3–GLIS2* have limited the investigation to AMKL and CN-AML patients in their characterization of fusion-positive cohorts, in part due to the low frequency of the fusion in unselected populations (~2%). Our study expands on the known features of fusion-positive AML by including a diverse cohort of patients encompassing all morphologic categories, in addition to normal cytogenetics and megakaryoblastic, to provide increased scope and detail in understanding the pathogenesis of this aggressive subtype. We identified 39 *CBFA2T3–GLIS2* fusion-positive cases from an unselected cohort of 2,027 pediatric AML patients, and all fusion-positive cases were experimentally validated using reverse-transcription (RT-PCR)-based methods. Available clinical annotations and flow cytometry data were interrogated, and finally, transcriptional profiling of mRNA and miRNA-sequencing data for 24 of 39 fusion-positive and 1,025 fusion-negative cases was used to identify fusion-specific molecular biomarkers from aberrantly expressed miRNAs, genes, and pathways. The specificity of these immunophenotypic and transcriptional markers can be leveraged to define a high-risk group of pediatric AML patients, who will need immediate and specialized treatment.

Materials and Methods

Biological specimens and clinical annotations

Pediatric patients with *de novo* AML enrolled on Children's Oncology Group (COG) trials CCG-2961, AAML03P1, AAML0531, and

AAML1031, with written informed consent and available clinical and/or molecular annotations, were included for biological study. Trials were conducted in accordance with the Declaration of Helsinki. The Fred Hutchinson Cancer Research Center Institutional Review Board and the COG Myeloid Biology Committee approved the study. Details of treatment protocols have been previously published (14–17). Analyses of outcome and clinical characteristics were limited to patients from AAML0531 and AAML1031. Data were current as of March 31, 2018, for outcome analyses, and cohort characteristics are summarized in Supplementary Tables S1 and S2. Patients with an FLT3-ITD high allelic ratio from AAML1031 were excluded from survival and clinical associations due to enrollment on the phase I sorafenib treatment arm, because a proportion of patients were still on therapy with data under DSMC review. Risk groups were defined as follows: patients with t(8;21), inv(16), NPM1 or CEBPA mutations were considered low risk, whereas patients with monosomy 7, monosomy 5/del5q, or high allelic ratio FLT3-ITD (ITD-AR > 0.4) were considered high risk (16). Remaining patients were considered standard risk. As a comparison, we screened 299 patients enrolled in the SWOG adult AML trial S0106.

Flow cytometry, cytotoxicity assays, and *CBFA2T3–GLIS2* transduction

Myeloid immune marker flow cytometry data were provided by Hematologics for 437 pediatric AML patients enrolled on AAML0531. Methods for flow cytometry were previously reported (18). Cytotoxicity assays were carried out on primary AML samples by Notable Labs translational drug-discovery platform and utilized the CD56 antibody clone m906 as previously described (19). The antibody controls included chKTI-SPP-DM1 (20) and human IgG-SAP and goat IgG-ZAP (Advanced Targeting Systems, #IT-36, #IT-35). Human cord blood samples were obtained with informed consent under Swedish Medical Center Institutional Review Board. CD34⁺ cord blood cells were transduced with a pRRL lentivirus encoding the *CBFA2T3–GLIS2* fusion transcript and GFP (21). Cell-surface antigen expression was assessed by flow cytometry (18).

RNA-sequencing library construction

RNA from primary patient samples was purified using the QIAcube system with AllPrep DNA/RNA/miRNA Universal Kits (QIAGEN, #80224). The mRNA libraries were prepared for 75-bp strand-specific paired-end sequencing using the ribodepletion 2.0 protocol by the British Columbia Genome Sciences Center (BCGSC, Vancouver, BC). Sequenced libraries were aligned to GRCh37, and gene-level coverage was quantified using the BCGSC pipeline v1.1 with Ensembl v69 annotations. The microRNA libraries were produced using the miRNA 3.0 protocol by BCGSC. Sequenced reads (31-bp) were trimmed to remove adapter sequences and aligned to GRCh37. Perfect alignments with no mismatches were retained for mature miRNA quantification using miRBase v20 annotations. Transcriptomic data are available through the dbGaP TARGET: AML study (accession: phs000465.v19.p8).

Screening of *CBFA2T3–GLIS2* fusion

The *CBFA2T3–GLIS2* fusion transcript was detected by RNA-sequencing for AAML1031 using STAR-fusion v1.1.0 and TransAbyss v1.4.10 fusion detection software (22, 23) and experimentally verified using RT-PCR. Patients enrolled on prior studies were screened by fragment length analysis (FLA) using the Applied Biosystems 3730xl DNA Analyzer. Primers for RT-PCR verification and FLA are listed in Supplementary Methods.

Differential expression, hierarchical clustering, gene set enrichment analysis, and miRNA-mRNA interactions

All analyses were completed in the R statistical environment. Differentially expressed genes and miRNAs were identified using Limma v.3.36.1, and those with absolute log₂ fold change > 1 and false discovery rate (FDR) < 0.05 were retained. Gene counts were TMM normalized and converted to log₂ scale for unsupervised hierarchical clustering. Gene set enrichment analysis was completed using GAGE v2.30.0 (24). Interactions between miRNA-mRNA were investigated by selecting pairs of differentially expressed miRNAs and genes with significant anti-correlation using Spearman's *rho* (FDR < 0.05). The miRNA-miRNA pairs were investigated for both predicted and validated interactions using anamiR v1.10.0 and multiMiR v1.4.0 packages. LNA inhibition of *miR-224* and *miR-452* in *CBFA2T3-GLIS2* M07E cells is described in Supplementary Methods.

Results

Fusion transcript detection

Primary samples from children and young adults enrolled on COG AAML1031 were utilized for RNA-sequencing, and the *CBFA2T3-GLIS2* fusion was identified using fusion detection algorithms (22, 23) and experimental validation by RT-PCR. Specimens from earlier studies were screened using RT-PCR-based methods (2). In total, we identified 39 fusion-positive cases from 2,027 patients screened (1.9%) with three distinct chromosomal breakpoints. The majority of fusion-positive patients (80%) had a breakpoint at exon 11 of *CBFA2T3* and exon 3 of *GLIS2* (Fig. 1A and B; ref. 25). The remaining had breakpoints between *CBFA2T3* exon 10 and *GLIS2* exon 2, and 1 patient was found to have a fusion breakpoint in *CBFA2T3* exon 9 and *GLIS2* exon 3 (Supplementary Fig. S1).

CBFA2T3-GLIS2 AML characteristics and clinical outcome

Complete clinical annotations were available for 37 fusion-positive and 1,724 fusion-negative cases from AAML0531 and AAML1031. All fusion-positive patients were < 3 years old, and the median age was 1.5 years (range, 0.75–2.96 years) compared with a median of 10.0 years for fusion-negative AML (range, 0.01–29.8 years, $P < 0.001$). In patients < 3 years of age, *CBFA2T3-GLIS2* fusion was seen in 8.4% (37/441) of cases, and the majority of *CBFA2T3-GLIS2* AML were diagnosed at 1-year-old, accounting for 11.7% of all patients diagnosed in this age group (Fig. 1C). In contrast, the *CBFA2T3-GLIS2* fusion was not detected in 299 adult patients with AML (ages 20–60 years, $P < 0.001$). There appears to be an ethnic predisposition for this fusion with nearly a third (29.4%) of *CBFA2T3-GLIS2* patients being black or African American, compared with 12.8% in the fusion-negative population ($P = 0.009$). Comparison of disease characteristics showed no significant difference in presenting white blood cell count at diagnosis between fusion-positive and negative patients.

All but one fusion-positive patient (97%) were classified as standard risk based on conventional cytogenetic or molecular characteristics (16). One patient was classified as favorable risk based on positive FISH for *Inv(16)* without corresponding karyotype. Previous detailed genomic evaluation of 9 fusion-positive cases by whole-genome, whole-exome, or targeted exome sequencing failed to show any recurrent somatic mutations (2).

Evaluation of the karyotype of *CBFA2T3-GLIS2* cases demonstrated presence of rare structural events in 63.9% of cases without any of the common AML-associated recurrent fusions. A single patient with *CBFA2T3-GLIS2* fusion was reported with *inv(16)* based on FISH but

lacked the karyotype and 1 patient was identified with *t(8;16)* by karyotype, without the supporting evidence of this translocation by RNA-seq fusion calls, leading one to consider this a potential genomic rearrangement that may not produce a translated fusion product. The genomic variant trisomy 3 was detected in 7 of 36 cases (19.4%) versus 13 (0.8%) cases among fusion-negative patients. A minority of fusion-positive cases had trisomy 21 (4/36, 11.1%, $P = 0.022$) and one with trisomy 8. The *CBFA2T3-GLIS2* fusion was also not seen in those with adverse karyotype including monosomy 7, monosomy 5, or deletion 5q. There was a modest enrichment of cytogenetically normal fusion-positive patients (33.3% CN-AML) compared with 22.6% CN for fusion-negative patients overall (Fig. 1D). Slightly greater than half of the fusion-positive cohort (18/33) had an M7 megakaryoblastic morphology ($P < 0.001$). The next most common FAB classification was M1 minimal differentiated morphology (6/33, 18.2%), whereas the remaining cases encompassed a variety of FAB types. The *CBFA2T3-GLIS2* fusion was also mutually exclusive of the *RBM15-MKL1* and *NUP98-KDM5A* fusions, despite both being prevalent in M7 megakaryoblastic and younger AML patients.

Morphologic response to induction chemotherapy was assessed for fusion-positive patients, revealing 50.0% morphologic CR rate at the end of induction 1 (EOI1) compared with 76.1% for fusion negative ($P < 0.001$). Fusion-positive AML had a higher median percentage of residual disease (MRD) at the end of induction 1 and 2 compared with the fusion-negative population; 80% were MRD positive at the end of induction 1 (vs. 26.7%, $P < 0.001$) and 35.5% at the end of induction 2 (vs. 13.7%, $P = 0.005$). In fact, 94.3% of *CBFA2T3-GLIS2* patients had detectable residual disease after induction 1 (median: 0.7%, range, 0.0%–41.0%). Overall survival (OS) at 5 years after study entry for *CBFA2T3-GLIS2* AML was 22.0% versus that of 63.0% in fusion-negative cases (HR = 2.8, $P < 0.001$, Fig. 1E). *CBFA2T3-GLIS2* was also associated with a higher probability of an event (death, relapse, or induction failure) with an event-free survival (EFS) at 5 years from study entry 18.9% versus 46.9% for fusion-negative patients (HR = 2.0, $P < 0.001$). Associated adverse prognostic impact was observed regardless of whether or not patients had megakaryocytic phenotype. A multivariable analysis including *CBFA2T3-GLIS2* status, cytogenetic/molecular risk classification, and M7 morphology demonstrated that *CBFA2T3-GLIS2* was an independent prognostic factor for both OS (HR = 2.3, $P < 0.001$) and EFS (HR = 2.0, $P = 0.005$; Supplementary Table S3). In addition, the *CBFA2T3-GLIS2* fusion has prognostic value independent of age (Supplementary Figs. S2 and S3). Infant AML patients ≤ 1-year-old with the *CBFA2T3-GLIS2* fusion ($N = 30$) had adverse OS compared with the fusion-negative ($N = 308$) population (27.6% vs. 61.3% at 5 years after enrollment, $P = 0.001$). Infant *CBFA2T3-GLIS2* patients with FAB M7 morphology ($N = 17$) remained at greater risk of death (OS 25%) compared with other FAB M7 infant AML cases ($N = 44$, OS 58.9%, $P = 0.025$) 5 years after study entry.

CBFA2T3-GLIS2 immunophenotype and targeted therapy

Evaluation of leukemic blast by multidimensional flow cytometry (MDF) demonstrated that leukemias with *CBFA2T3-GLIS2* had a highly elevated CD56 expression, that in combination with dim or absent expression of HLA-DR, CD38, and CD45 can be characterized as previously described RAM phenotype (18). All patients with *CBFA2T3-GLIS2* fusions were evaluated by MDF and were found to have RAM phenotype (100%, $P < 0.001$). Expression values for 13 cell-surface antigens (myeloid marker panel) by MDF were available for a subset of patients from AAML0531 ($N = 437$). Unsupervised hierarchical clustering demonstrated that fusion-positive tumors (7/7)

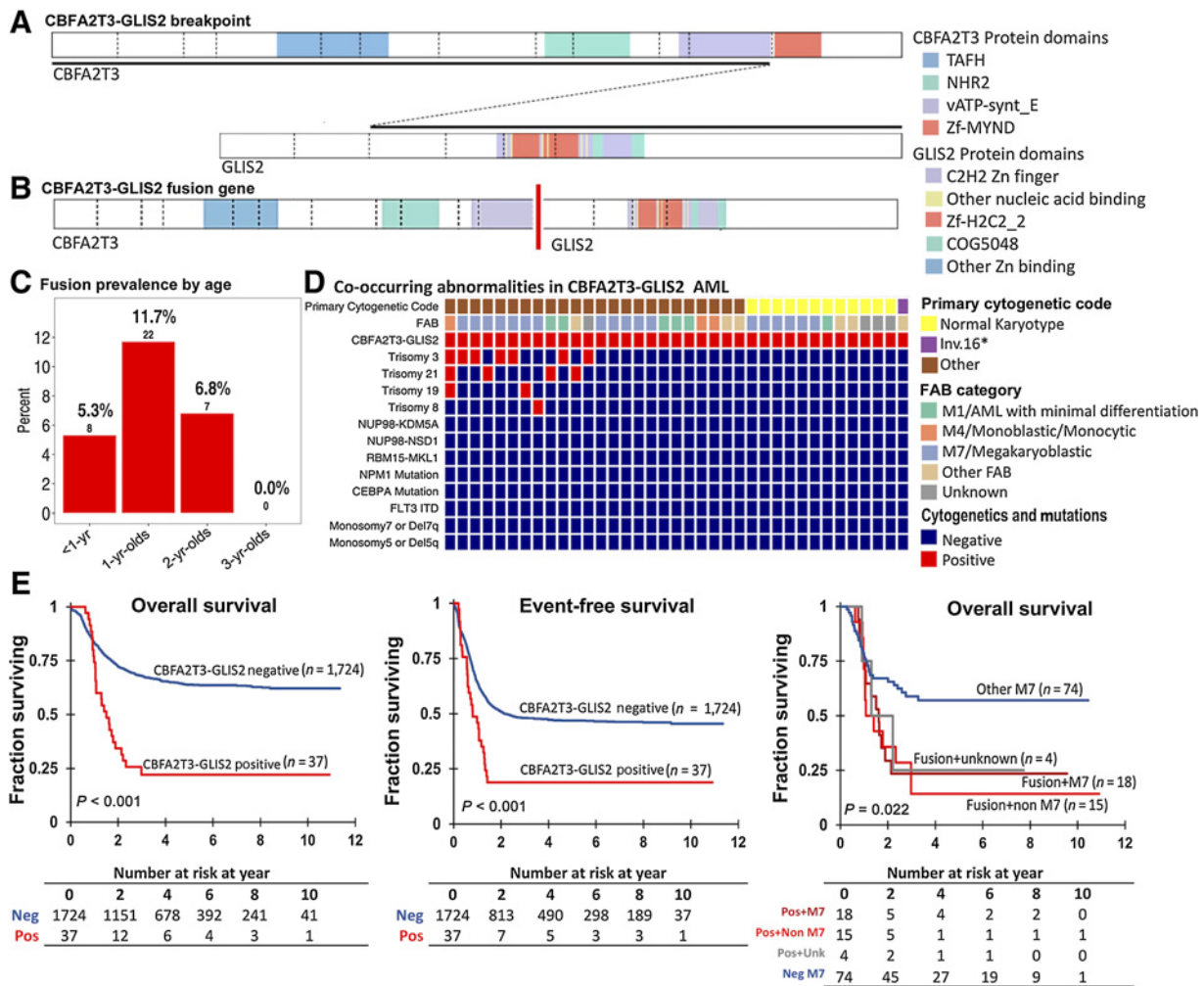


Figure 1.

The cryptic fusion *CBFA2T3-GLIS2* is most prevalent in patients less than 3 years old and is associated with poor outcomes. **A**, Representation of the most common breakpoint in pediatric AML (Zhou and colleagues; ref. 25) and **B** resulting in the *CBFA2T3-GLIS2* fusion transcript. **C**, Frequency of *CBFA2T3-GLIS2* occurrence by age group. **D**, OncoPrint with the *CBFA2T3-GLIS2* cohort. Columns show patients, and genetic abnormalities are shown in rows. *, One patient (purple) was identified as inv(16) through FISH, though no RNA-seq or karyotype evidence was detected. **E**, Kaplan-Meier estimates for *CBFA2T3-GLIS2* AML compared with fusion-negative cohorts.

clustered together by mean fluorescence intensity (MFI) of the 13 antigens, indicating that *CBFA2T3-GLIS2* tumors have highly distinctive immunophenotypes, with extremely elevated surface CD56 expression ($P < 0.001$, Fig. 2A; Supplementary Fig. S4). We also evaluated the available diagnostic immunophenotype data to determine whether fusion-positive cases could be identified using the characteristic RAM phenotype antigens: CD56, CD45, CD38, and HLA-DR. Unconstrained classic metric multidimensional scaling (MDS) was used to cluster the 437 patients using MFI values of the four RAM antigens, and observed 100% (7/7) of fusion-positive AML patients clustered away from the fusion-negative cohort, providing compelling evidence that *CBFA2T3-GLIS2* is associated with a unique cell-surface expression profile that can be characterized by the RAM antigens alone (Fig. 2B).

Next, considering that a majority of *CBFA2T3-GLIS2* patients express the RAM immunophenotype, we investigated whether transcript-level expression would support the observations of low-to-

dim expression of CD45, CD38, and HLA-DR. Using rRNA-depleted RNA-sequencing data from 24 fusion-positive cases, it was found both *CD38* and *CD45* transcripts were significantly down-regulated > 2 -fold compared with fusion-negative AML ($N = 1,025$), as well as the HLA-DR genes: *HLA-DRA*, *HLA-DRB1*, *HLA-DRB5*, and *HLA-DRB6* (FDR < 0.001). Investigation of miRNA-mRNA interactions using paired miRNA-sequencing data revealed *CD38* mRNA had significant anti-correlation (Spearman's ρ) and predicted target binding sites for the overexpressed *miR-203a-3p* ($r_s \leq -0.62$, FDR = 0.02). For *CD45*, there were significant associations with highly expressed mature *miR-452-3p*, *miR-425-5p*, and both *miR-224* species ($r_s \leq -0.74$, FDR ≤ 0.003). HLA-DR genes also had relationships with overexpressed miRNAs: *HLA-DRA* had predicted target sites for *miR-135a-3p* ($r_s = -0.62$, FDR = 0.02) and *HLA-DRB5* with *miR-5683* ($r_s = -0.53$, FDR < 0.05), thus implicating miRNAs in negative regulation of the cell-surface markers that define the RAM phenotype.

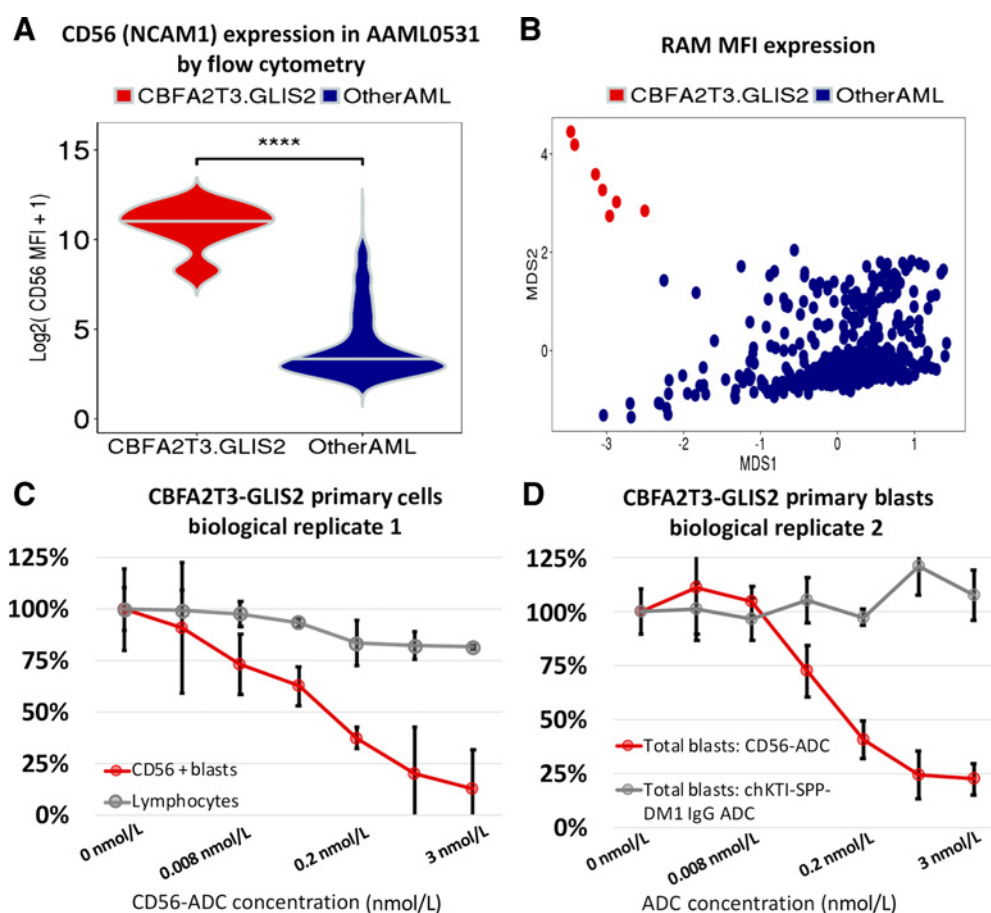


Figure 2.

Fusion-positive cases highly overexpress surface CD56 (NCAM1), and targeting CD56 with an antibody–drug conjugate results in greater than 75% cytotoxicity. **A**, CD56 (NCAM1) surface expression by flow cytometry in MFI values in *CBFA2T3–GLIS2* patient samples ($N = 7$) from AAML0531. **B**, Classic metric multidimensional scaling using expression of CD56, HLA-DR, CD38, and CD45 antigens' MFI values. **C**, Cytotoxicity assay with *CBFA2T3–GLIS2* primary cells from biological replicate #1. Blasts and normal lymphocytes from the patient were exposed *in vitro* to varying concentrations of the CD56 ADC in triplicate. **D**, Cytotoxicity assay with *CBFA2T3–GLIS2* blasts exposed to either the nontargeting conjugate control, chKTI-SPP-DM1 IgG ADC, or CD56-ADC. Each condition and concentration were completed in triplicate.

We next evaluated CD56 as a potential therapeutic target using an anti-CD56 antibody–drug conjugate (m906-PBD-ADC) developed by the NCI (19, 20). Leukemic blasts and control lymphocytes from a patient with relapsed fusion-positive AML were incubated with varying doses of m906, and cytotoxicity was assessed after 72 hours. The CD56-ADC exhibited a dose-dependent and CD56-specific toxicity on leukemic blasts. There was 87% cytotoxicity of CD56⁺ blasts at 3 nmol/L concentration, suggesting that CD56 might prove to be a therapeutic target in this high-risk cohort of patients ($P < 0.001$, Fig. 2C). The CD56-ADC was further evaluated in an additional 3 independent *CBFA2T3–GLIS2* patient samples; the dose-dependent toxicity was observed in all samples. In total, 3 of 4 *CBFA2T3–GLIS2* primary samples showed > 75% cytotoxicity of leukemic blasts at 3 nmol/L concentration of the CD56-ADC (Fig. 2D; Supplementary Fig. S5).

Malignant transformation of cord blood stem cells by *CBFA2T3–GLIS2* fusion

Given the paucity of cooperating events in a highly aggressive disease in early life, we questioned whether this fusion may be sufficient for malignant transformation. To this end, we transduced

human CD34⁺ cord blood stem cells (CBSC) with a lentivirus encoding the *CBFA2T3–GLIS2* fusion transcript and GFP or mock control; expression of the fusion was confirmed by RT-PCR. Fusion-transduced CBSCs were more proliferative compared with mock-transduced CBSCs (Supplementary Fig. S6, $P = 0.21$). After 12 weeks in culture, we evaluated immunophenotypic and morphologic features of *CBFA2T3–GLIS2* fusion-transduced cells. *CBFA2T3–GLIS2*⁺ cells had immature morphology with high CD117 expression and absence of CD11b, CD36, and CD64 (Fig. 3A and C). Of significance, fusion-transduced cells had remarkably high CD56 expression (3,556 MFI vs. 43 MFI for the control), similar to that observed in patients with fusion-positive RAM phenotype (2,040 MFI), suggesting that CD56 expression is causally linked to the expression of the fusion transcript. In addition, morphologic evaluation of *CBFA2T3–GLIS2*⁺ cells revealed multinucleated cells, prominent nucleoli, and abundant focally basophilic and vacuolated cytoplasm with cytoplasmic blebs, which are morphologic features suggestive of megakaryocytic differentiation. Megakaryocytic lineage was confirmed by demonstration of high expression of CD41 and CD61 on the surface of transduced cells (Fig. 3D and E).

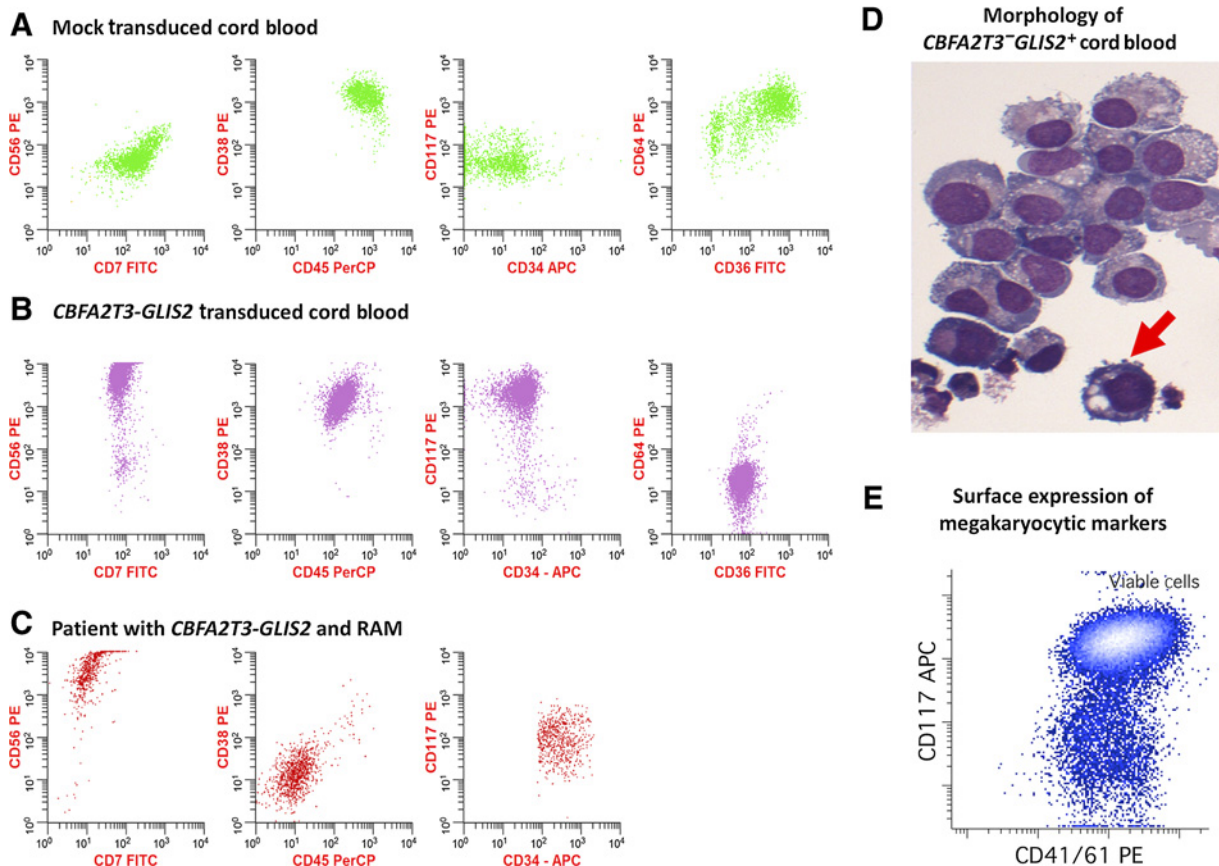


Figure 3.

CBFA2T3-GLIS2 induces overexpression of CD56 (NCAM1) in healthy normal cord blood cells. **A**, Surface immunophenotype of mock-transduced cord blood cells cultured for 6 weeks (green); **B**, *CBFA2T3-GLIS2* transduced cord blood cells cultured for 10 weeks (purple), and **C** patient with *CBFA2T3-GLIS2* and RAM phenotype (red). Patient data for CD64 and CD36 are not available. Morphology of *CBFA2T3-GLIS2*-transduced cells includes **D** megakaryocytic features, such as cytoplasmic blebs, noted with arrow, and **E** cells express megakaryocytic surface markers CD41 and CD61.

Gene-expression profiling of *CBFA2T3-GLIS2* patients

Of 39 pediatric *CBFA2T3-GLIS2* AML patients identified, 24 of 39 fusion-positive and 1,025 fusion-negative cases had material available for high depth ribodepleted mRNA-sequencing and paired miRNA-sequencing. Transcriptome data from *CBFA2T3-GLIS2*-positive and -negative tumors were contrasted to identify fusion-specific pathways, genes, and miRNAs (Fig. 4A). Gene set enrichment analysis (24) identified a substantial activation of Hippo (FDR < 0.001) and TNF signaling pathways (FDR < 0.001), which have been implicated in various cancers by promoting cellular functions that enhance tumor growth, migration, and proliferation (26, 27). In addition, TGF β /BMP and Hedgehog signaling pathways showed significant activation, as previously identified (refs. 3, 6; FDR \leq 0.001, Fig. 4B and C). Furthermore, the cell-surface NCAM1 (CD56) interaction pathway was highly positively enriched (FDR < 0.001), whereas gene-ontology (GO) term analysis revealed significant upregulation of numerous cell adhesion and cell-surface marker genes, including extracellular matrix binding, cell-adhesion molecule binding, and integrin binding genes (FDR < 0.001).

Considering that a characteristic feature of *CBFA2T3-GLIS2* AML was positive regulation of cell adhesion and extracellular matrix binding (ECM), overexpressed genes whose protein products have demonstrated localization to the plasma membrane and ECM were

examined (28). Of 3,711 differentially expressed genes (DEG), 789 genes had cell adhesion, plasma membrane, and ECM associations (FDR < 0.001, Fig. 5A; Supplementary Fig. S7). Plasma membrane and ECM genes included 10 NCAM1 interaction pathway genes, overexpressed hematopoietic lineage adhesion molecules CD44, ITGA2, and ITGA2B, as well as numerous receptor tyrosine kinases. CD44, expressed at a level more than 2-fold greater than fusion-negative patients, is aberrantly expressed on leukemic stem cells and a marker of HSCs (29, 30). Similarly, ITGA2 is a cell adhesion molecule on hematopoietic cells and used to classify subsets of HSCs (29). Upregulated receptor tyrosine kinases (RTK) that localize to the cell periphery and cell membrane included ROR1, MET, NTRK1, and two of the TAM family kinases, TYRO3 and AXL, were noted [log2 fold change (LFC) \geq 2.0, FDR < 0.001]. The TAM family of RTKs has been shown to increase tumor cell survival, migration, and chemoresistance (31), whereas others have known roles in cancer progression (32, 33). In addition, genes affected by BMP and hedgehog signaling cross-talk (10) with demonstrated ECM localization were upregulated, including BMP2, WNT9A, and WNT11. A concomitant overexpression of WNT11 and ERG transcripts (LFC \geq 1.5, FDR < 0.001) was observed, and it has been shown that the ERG transcription factor directly binds the WNT11 locus to promote cancerous transformation in AML (34).

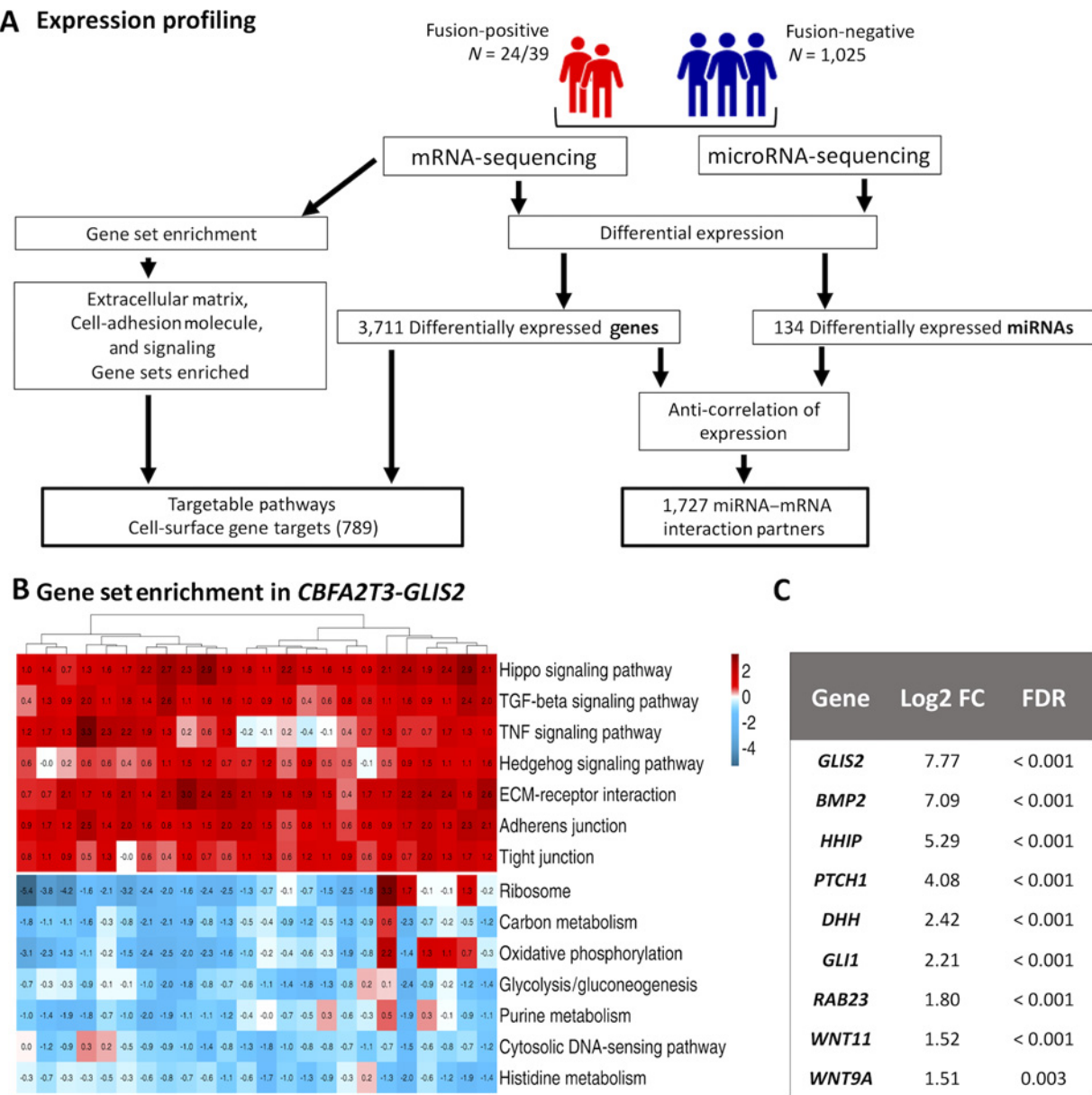


Figure 4. A cohort of 24 *CBFA2T3-GLIS2* AML patient samples was used in transcriptional profiling for mRNA and miRNA differential expression analysis and gene set enrichment analysis. **A**, Schematic representation of the data types and transcriptomic analyses in this study. **B**, Heat map of positively and negatively (blue) enriched pathways from gene set enrichment analysis of the *CBFA2T3-GLIS2* cohort. Pathways (rows) have Benjamini-Hochberg-adjusted *P* values ≤ 0.001 . The enrichment statistic for the gene set enrichment analysis is denoted in each tile and was derived from a two-sample *t* test for differential expression of gene sets. **C**, Differentially expressed genes involved in Hedgehog signaling or its cross-talk found to be upregulated in *CBFA2T3-GLIS2* tumors.

Unsupervised hierarchical clustering based on the most highly expressed (90th percentile LFC, *N* = 79 genes) cell surface-associated genes found *CBFA2T3-GLIS2* AML exhibits a unique expression profile with a distinct set of dysregulated genes: *NCAM1* (CD56), the *NCAM1*-interacting partner *CACNB2*, and *GABRE* receptor gene (Fig. 5B). Hierarchical clustering on the cell adhesion/ECM-associated markers also revealed a number of fusion-negative AML patients (*N* = 66) that clustered closely with the fusion-positive cohort. This cohort shared similar characteristics with fusion-positive patients: they tend to be very young, with a median age of 1.8 years

(range, 0.09–17.6 years) and 85% of cases are < 3 years old. They were enriched in M7 AML (*N* = 37/54, 68%), including the majority of *NUP98-KDM5A* (*N* = 12/17, 70.5%) and *RBM15-MKL1* (*N* = 10/10, 100%) cases. Patients with similar cell-surface associated gene expression also had poor outcomes compared with the fusion-negative population for OS (47.5% vs. 64.8%, *P* < 0.001), though not EFS (*P* = 0.17). Identification of similar patients allows the inclusion of many AML patients that otherwise would be missed in a targeted investigation of therapeutic biomarkers. However, these patients have some distinct differences, sharing 57 of 79 (72%) of the most upregulated cell

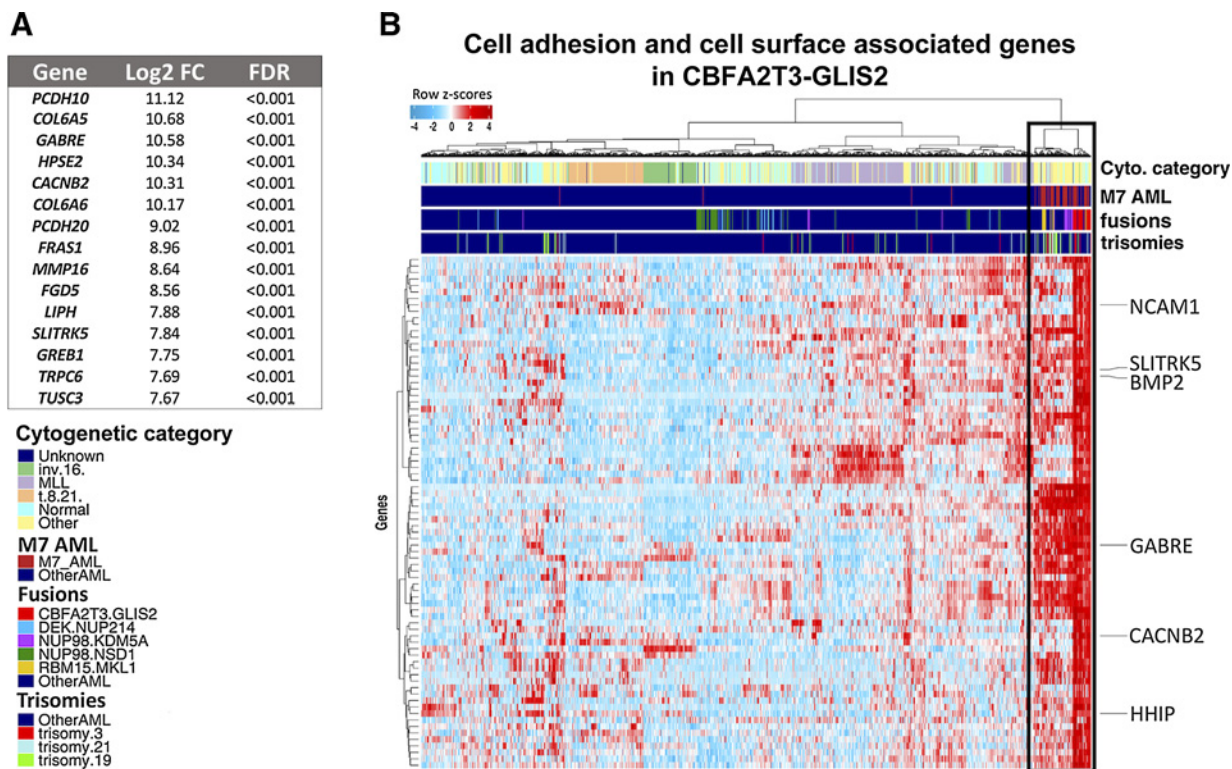


Figure 5. *CBFA2T3-GLIS2* cases overexpress a number of cell-adhesion, cell-surface, and extracellular matrix-associated genes. **A**, Top 15 significantly upregulated cell adhesion, extracellular matrix, and cell surface-associated genes in *CBFA2T3-GLIS2* AML. **B**, Unsupervised hierarchical clustering of 1,049 pediatric AML patients using the 90th percentile of highest upregulated cell-surface genes (FDR < 0.001). Color bars indicate primary cytogenetic code, M7 AML classification, fusion status (*CBFA2T3-GLIS2* in red), and trisomies associated with *CBFA2T3-GLIS2*. The patients with similar cell-adhesion/extracellular matrix-associated gene expression profiles are highlighted by the black box.

surface-associated genes in common with *CBFA2T3-GLIS2* (Supplementary Table S4).

MicroRNA profiling of *CBFA2T3-GLIS2* patients

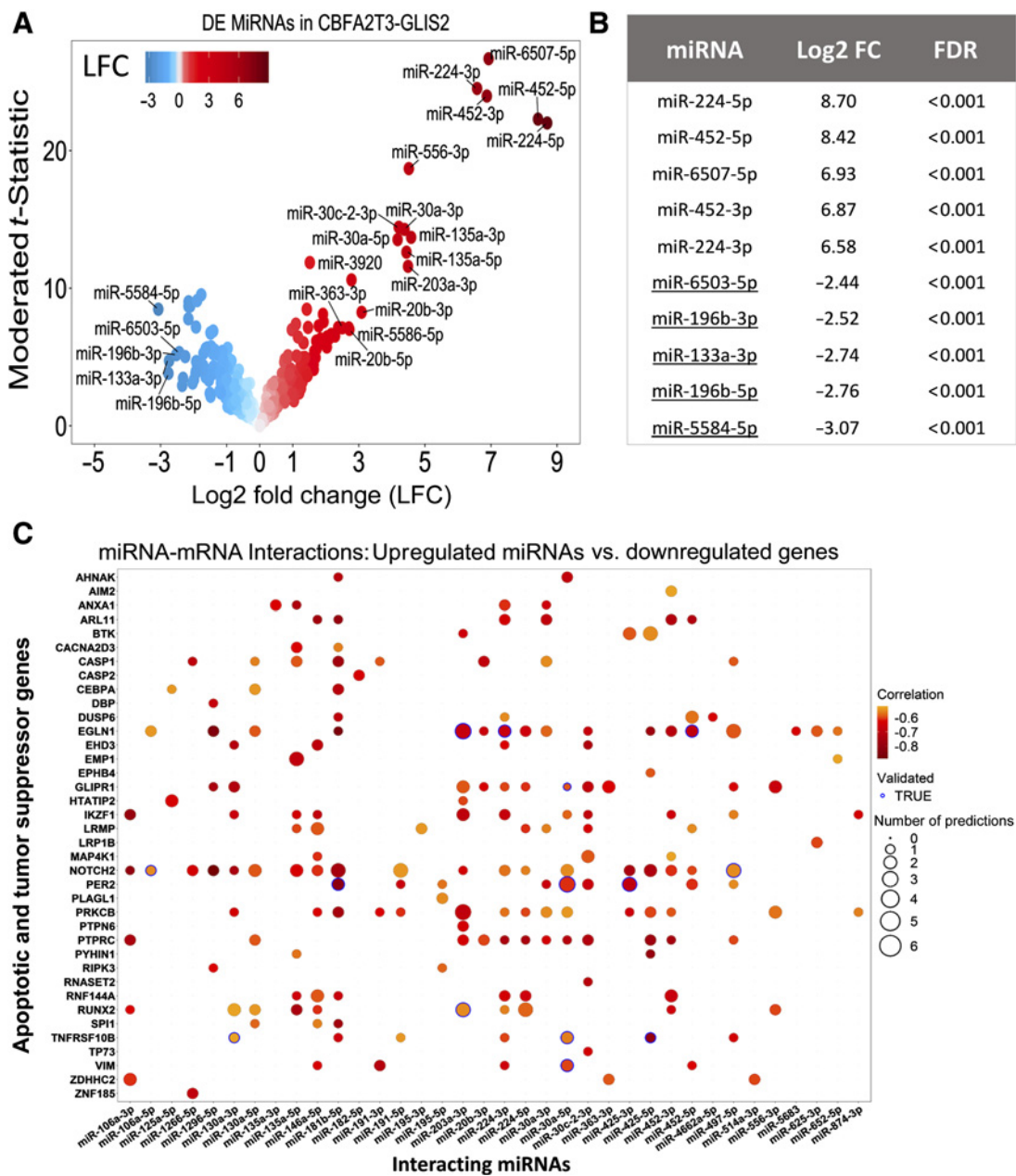
The 1,049 patients with whole-transcriptome data had paired miRNA-sequencing completed. Contrasting *CBFA2T3-GLIS2* AML ($N = 24$) against the fusion-negative cohort ($N = 1,025$) revealed 134 differentially expressed mature miRNAs, with the magnitude of differential expression being much greater for the upregulated miRNAs (Fig. 6A). The most highly expressed miRNAs were *miR-224-5p*, *miR-224-3p*, *miR-452-5p*, *miR-452-3p*, and *miR-6507-5p* (Fig. 6B). Human *miR-224* and *miR-452* have both been implicated as oncomirs in malignant melanoma, as well as colorectal cancers, and are intronic miRNAs transcribed from the *GABRE* locus, one of the most highly aberrantly expressed cell membrane-associated genes in *CBFA2T3-GLIS2* (35, 36). Conversely, the most downregulated miRNAs were *miR-6503-5p*, *miR-196b-3p*, *miR-196b-5p*, *miR-133a-3p*, and *miR-5584-5p*. The mature miRNA *miR-196b* functions as a tumor suppressor during lung carcinogenesis (37), and well-characterized *miR-133a* has been found to function in a tumor-suppressive manner in as many as five cancers, including breast and colorectal cancer (38).

To examine miRNA regulatory networks in *CBFA2T3-GLIS2*, miRNA-mRNA interactions were investigated by selecting significantly anti-correlated differentially expressed miRNA-gene pairs (Spearman's ρ , FDR < 0.05). The miRNA-gene pairs were queried across independent target-prediction and experimental evidence data-

bases, identifying 1,727 miRNA-mRNA interacting partners. Predicted interactions were only considered if two or more algorithms identified the miRNA binding-site homology or the interaction was supported by experimental evidence. The most highly overexpressed miRNAs in *CBFA2T3-GLIS2* tumors, *miR-224* and *miR-452*, were associated with numerous mRNA targets. GO enrichment analysis of *miR-224* target genes ($N = 107$ genes) revealed that these were involved in immune response (FDR = 0.002) and leukocyte activation (FDR = 0.005), indicating these pathways are inhibited in fusion-positive AML and high expression of *miR-224* potentially contributes to the pathways' modulation. The overexpressed mature *miR-452* associated with 127 target genes, which are involved in leukocyte differentiation (FDR = 0.001), and immune system processes (FDR = 0.001), as well as myeloid leukocyte differentiation (FDR = 0.02). A perturbation experiment using LNA miRNA inhibitors for (i) *hsa-miR-224-5p*, (ii) *hsa-miR-224-3p*, (iii) *hsa-miR-452-5p*, or (iv) *hsa-miR-452-3p* was performed. The *CBFA2T3-GLIS2* cell line MO7E was exposed to inhibitor for 72 hours, resulting in a knockdown efficiency > 90% for each miRNA (Supplementary Fig. S8). Proliferation rates were assessed for the following 4 days (7 days of continuous LNA inhibitor exposure). The inhibition of each miRNA alone produced minimal to no morphologic or immunophenotypic alterations and led to subtle increase in proliferation compared with negative control inhibitors (Supplementary Fig. S9; $P \leq 0.01$).

In contrast to gaining proliferative ability, tumors' modulation of apoptotic genes is often involved in cancer progression (39). Two such

Downloaded from http://aacrjournals.org/clincancerres/article-pdf/26/3/726/206536/1726.pdf by Fred Hutchinson Cancer Center user on 08 October 2024



genes, *CASP1* and *TRAIL-R2*, were significantly downregulated, as well as the tumor suppressors *GLIPR1* and *PER2* (39–41). *CASP1* was significantly anti-correlated with, and a putative target of the overexpressed *miR-181b-5p* ($r_s = -0.76$, FDR = 0.002, Fig. 6C). *TRAIL-R2* associated with upregulated mature *miR-425-5p*, and the regulatory interaction had experimentally validated evidence ($r_s = -0.80$, FDR < 0.001). *GLIPR1* mRNA decreased with increasing *miR-130a-3p* transcript levels ($r_s = -0.72$, FDR = 0.003) and *PER2* displayed significantly anti-correlated expression levels with *miR-*

181b-5p ($r_s = 0.82$, FDR < 0.001) and possessed experimental evidence of the interaction.

Finally, we investigated regulatory interactions among the most significantly downregulated miRNAs in CBFA2T3-GLIS2 AML. Mature *miR-196b-5p* had an identified regulatory interaction with the cell adhesion molecule *ITGA2*, whose expression was 22-fold greater in fusion-positive AML ($r_s = -0.75$, FDR = 0.03). *ITGA2* is expressed on HSCs (29), and silencing of *miR-196b* appears to induce abnormal regulation of this marker. In addition, *miR-196-5p* had target

binding sites identified within DNA methyltransferase *DNMT3B* transcripts ($r_s = -0.73$, FDR = 0.03). *DNMT3B* was upregulated in *CBFA2T3–GLIS2* tumors and has been associated with adverse outcome in pediatric AML (42). The *miR-199a/b* family members, characterized as tumor suppressors in multiple cancers including AML (43, 44), had a predicted regulatory relationship with the massively overexpressed plasma-membrane *SLITRK5* gene (over 200-fold more highly expressed in fusion-positive cases, FDR < 0.001). *SLITRK5*, expressed on both HSCs and aberrantly on CD34⁺ leukemic cells (45), had a predicted binding site for *miR-199b-3p* and *miR-199a-3p* ($r_s \leq -0.73$, FDR ≤ 0.03), thus providing one putative mechanism contributing to the overexpression of this AML-associated gene transcript (Supplementary Fig. S10).

Discussion

This comprehensive study represents a large uniformly treated cohort of patients to be evaluated by transcriptome sequencing, in order to define the biological implications of the *CBFA2T3–GLIS2* fusion in children with *de novo* AML. We established that although the prevalence of *CBFA2T3–GLIS2* is ~2% across an unselected pediatric cohort, it is highly enriched in younger AML populations (5, 46, 47), with nearly 12% of 1 year-old infants harboring this fusion. In fact, the *CBFA2T3–GLIS2* fusion was not detected in those older than 3 years of age. We also confirmed the *CBFA2T3–GLIS2* fusion is not limited to those with AMKL or normal karyotypes (3–7), with predilection to patients with African ancestry. Further, a majority of *CBFA2T3–GLIS2* positive patients have nonrecurrent karyotypic alterations with unexplained enrichment of trisomy 3, and the overwhelming majority express the unique RAM immunophenotype, which provides a seamless mechanism for rapid identification of this high-risk population (18).

Furthermore, the lack of recurrent fusions or somatic mutations in a very young population suggests that this cryptic fusion may be sufficient for leukemic transformation without requirement for additional cooperating events. We confirmed this hypothesis by demonstrating that transduction of CBSC leads to malignant transformation that recapitulates infant AML with enhanced proliferation, maturation arrest, as well as morphologic and immunophenotypic alterations consistent with megakaryocytic AML. This is in contrast to the disease in older patients where cooperation between class I and II variants is required for malignant transformation (48). The fact that transduction of CBSC led to induction of NCAM1 (CD56) expression, in combination with the previously published data that the fusion protein directly binds to the *NCAM1* promoter (4, 13), provides substantial evidence that CD56 expression is causally and directly related to the fusion and suggests that effective targeting of CD56 may be curative.

In addition, this subgroup displayed unique transcriptional dysregulation compared with other AML groups. Similar to findings reported in AMKL, significant activation of the hedgehog (HH) and TGF β /BMP signaling pathways was observed in *CBFA2T3–GLIS2* AML across all FAB and cytogenetic classifications, and exhibited upregulation of the canonical HH genes *PTCH1*, *HHIP*, and *GLI1* and the downstream target *BMP2* (3–6). The HH and BMP pathways are known to interact with each other, and their cross-talk has been implicated in multiple cancers (10, 26, 27). This finding provides further evidence that the *CBFA2T3–GLIS2* fusion is accompanied by dysregulation of hedgehog signaling, and that this pathway may contribute to the proliferative capacity of leukemic cells in AML. Gene-expression profiling also revealed a cohort of fusion-negative patients who cluster closely with *CBFA2T3–GLIS2* true positive cases,

and this signature identifies a larger cohort of patients with a shared expression profile of cell surface-associated genes. This may be especially important for other high-risk fusions such as *NUP98–KDM5A*.

In order to unravel the complex regulatory networks that are involved in the transcriptional dysregulation of *CBFA2T3–GLIS2*, we investigated the expression of mature miRNAs in fusion-positive AML. The most highly upregulated miRNAs were *miR-224* and *miR-452*, which have been shown to be associated with poor outcomes across six independent colorectal cancer cohorts, and both are overexpressed in malignant melanoma (35, 36). Interestingly, target genes of *miR-224* and *miR-452* were associated with GO enrichment of immune system processes and leukocyte differentiation, suggesting a possible mechanism of an immunosuppressive environment in fusion-positive AML. It was also demonstrated that *miR-224/miR-452* genes are located in a miRNA cluster and are induced by transactivation of *GABRE*, which was one of the most highly upregulated genes in *CBFA2T3–GLIS2* (LFC = 10.6, FDR < 0.001; ref. 35). However, the evidence suggested overexpression of E2F1 drove transactivation, yet *CBFA2T3–GLIS2* AML lacked an overexpression of E2F1, suggesting an alternative mechanism of regulation. Transcription factor binding sites in K562 ChIP-seq from the ENCODE project showed that TAL1 and RBFOX2, both upregulated > 2-fold in *CBFA2T3–GLIS2* patients, bind to the promoter region of *GABRE*, indicating alternative avenues for the observed overexpression (49). The results of the knockdown experiments are more difficult to interpret, and may indicate that these miRNAs may not be limited to enhancing cell-division/mitotic potential, but offer an alternative clonal advantage, possibly related to cell quiescence considering their apparent negative regulation of proliferation. In addition, it cannot be discounted that inhibition of these closely related miRNAs individually may not account for potential synergistic effects. Combinatorial inhibition experiments may provide improved elucidation of the regulatory mechanisms to which the four miRNAs contribute.

Alternatively, many upregulated miRNAs in fusion-positive AML were found to target apoptotic and tumor suppressor genes; *miR-181b-5p* was highly elevated in *CBFA2T3–GLIS2* tumors and had predicted target sites on the downregulated apoptotic genes *CASP1* and *TRAIL-R2*, and the circadian rhythm gene *PER2*. Meanwhile, tumor-suppressive miRNAs, including *miR-196a/b*, *miR-133a*, and *miR-199a/b*, had significantly reduced expression in fusion-positive AML, suggesting another mode for tumor progression. Upregulation of *ITGA2* and *DNMT3B*, which have been shown to be independent prognostic indicators associated with poor outcomes in AML when highly expressed, were associated with the loss of *miR-196b* expression (42, 50). Taken together, this suggests another means for leukemic tumor cells to deregulate normal signals for cell growth arrest.

In summary, *CBFA2T3–GLIS2* fusion is a highly potent fusion oncogene that is sufficient for malignant transformation and induction of highly refractory leukemia. Identification of this fusion early at diagnosis would allow more appropriate risk adaptive therapeutic intervention. Although at present targeted therapies are not available for these highly refractory patients, identification of causal association of the fusion oncogene and surface CD56 expression provides a viable target that may be curative. The promising results of the CD56-ADC across 4 independent primary samples demonstrated the potency and specificity of this therapeutic strategy. Targeting the CD56 antigen offers the most immediately actionable target in this cohort of high-risk patients, and an effective CD56-ADC with limited off-target toxicity is available for continued refinement toward this goal. Additionally, this study provides comprehensive transcriptome profiling of *CBFA2T3–*

GLIS2 patients who defines an expression signature and dysregulated pathways and networks in this distinct and highly lethal AML of infancy. The vast body of data generated defining fusion oncoprotein-mediated alterations that lead to therapeutic resistance can be used for the development of precisely directed targeted therapies.

Disclosure of Potential Conflicts of Interest

M.T. Santaguida is an employee/paid consultant for Notable Labs. L.E. Brodersen is an employee/paid consultant for Hematologics. L. Pardo is an employee/paid consultant for Hematologics. M.R. Loken is an employee/paid consultant for and holds ownership interest (including patents) in Hematologics. No potential conflicts of interest were disclosed by the other authors.

Authors' Contributions

Conception and design: J.L. Smith, L.E. Brodersen, Q. Le, S. Meshinchi

Development of methodology: K.R. Loeb, Q. Le, S. Imren, T.J. Triche Jr, D. Meerzaman, H. Bolouri, S. Meshinchi

Acquisition of data (provided animals, acquired and managed patients, provided facilities, etc.): M.T. Santaguida, L.E. Brodersen, C.L. Cummings, K.R. Loeb, A.S. Gamis, R. Aplenc, M.R. Loken, S. Meshinchi

Analysis and interpretation of data (e.g., statistical analysis, biostatistics, computational analysis): J.L. Smith, R.E. Ries, T.A. Alonzo, R.B. Gerbing, L.E. Brodersen, C.L. Cummings, K.R. Loeb, S. Imren, R. Aplenc, J.E. Farrar, T.J. Triche Jr, C. Nguyen, D. Meerzaman, M.R. Loken, V.G. Oehler, H. Bolouri, S. Meshinchi

Writing, review, and/or revision of the manuscript: J.L. Smith, R.E. Ries, T.A. Alonzo, R.B. Gerbing, L.E. Brodersen, C.L. Cummings, A.R. Leonti,

A.S. Gamis, R. Aplenc, E.A. Kolb, J.E. Farrar, D. Meerzaman, V.G. Oehler, H. Bolouri, S. Meshinchi

Administrative, technical, or material support (i.e., reporting or organizing data, constructing databases): T. Hylkema, C.L. Cummings, E.A. Kolb, S. Meshinchi

Study supervision: A.S. Gamis, E.A. Kolb, D. Meerzaman, S. Meshinchi

Other (analysis of flow cytometry data): L. Pardo

Acknowledgments

This work utilized the computational resources of Fred Hutchinson Cancer Research Center (FHCRC) Scientific Computing and the NIH HPC Biowulf cluster (<http://hpc.nih.gov>). Sequencing of the AAML1031 cohort was supported by Target Pediatric AML (TpAML, <https://targetpediatricaml.org/>). Additional funding was provided by St. Baldrick's Consortium Grant, Bayer HealthCare Pharmaceuticals, Inc., and the Children's Oncology Group Foundation. This study was supported by R01CA 114563-10 (S. Meshinchi), COG Chair's Grant (U10CA098543), NCTN Statistics and Data Center (U10CA180899), NCTN Operations Center Grant (U10CA180886), Andrew McDonough B+ Foundation (AMBF), St. Baldrick's Foundation (SBF), Target Pediatric AML (TpAML), COG Foundation, HHSN261200800001E (S. Meshinchi), Project Stella (S. Meshinchi), and Hyundai Hope on Wheels (S. Meshinchi).

The costs of publication of this article were defrayed in part by the payment of page charges. This article must therefore be hereby marked *advertisement* in accordance with 18 U.S.C. Section 1734 solely to indicate this fact.

Received June 25, 2019; revised October 9, 2019; accepted November 7, 2019; published first November 12, 2019.

References

- Schuback HL, Arcaci RJ, Meshinchi S. Somatic characterization of pediatric acute myeloid leukemia using next-generation sequencing. *Semin Hematol* 2013;50:325–32.
- Bolouri H, Farrar JE, Triche T Jr, Ries RE, Lim EL, Alonzo TA, et al. The molecular landscape of pediatric acute myeloid leukemia reveals recurrent structural alterations and age-specific mutational interactions. *Nat Med* 2018;24:103–12.
- Gruber TA, Larson Gedman A, Zhang J, Koss CS, Marada S, Ta HQ, et al. An Inv (16)(p13.3q24.3)-encoded CBFA2T3-GLIS2 fusion protein defines an aggressive subtype of pediatric acute megakaryoblastic leukemia. *Cancer Cell* 2012;22:683–97.
- Thiollier C, Lopez CK, Gerby B, Ignacimoutou C, Poglio S, Duffourd Y, et al. Characterization of novel genomic alterations and therapeutic approaches using acute megakaryoblastic leukemia xenograft models. *J Exp Med* 2012;209:2017–31.
- Masetti R, Pigazzi M, Togni M, Astolfi A, Indio V, Manara E, et al. CBFA2T3-GLIS2 fusion transcript is a novel common feature in pediatric, cytogenetically normal AML, not restricted to FAB M7 subtype. *Blood* 2013;121:3469–72.
- de Rooij JD, Branstetter C, Ma J, Li Y, Walsh MP, Cheng J, et al. Pediatric non-down syndrome acute megakaryoblastic leukemia is characterized by distinct genomic subsets with varying outcomes. *Nat Genet* 2017;49:451–6.
- Hara Y, Shiba N, Ohki K, Tabuchi K, Yamato G, Park MJ, et al. Prognostic impact of specific molecular profiles in pediatric acute megakaryoblastic leukemia in non-Down syndrome. *Genes Chromosomes Cancer* 2017;56:394–404.
- Kim YS, Kang HS, Jetten AM. The Kruppel-like zinc finger protein Glis2 functions as a negative modulator of the Wnt/beta-catenin signaling pathway. *FEBS Lett* 2007;581:858–64.
- Lamar E, Kintner C, Goulding M. Identification of NKL, a novel Gli-Kruppel zinc-finger protein that promotes neuronal differentiation. *Development* 2001;128:1335–46.
- Bertrand FE, Angus CW, Partis WJ, Sigounas G. Developmental pathways in colon cancer: crosstalk between WNT, BMP, Hedgehog and Notch. *Cell Cycle* 2012;11:4344–51.
- Ingham PW, McMahon AP. Hedgehog signaling in animal development: paradigms and principles. *Genes Dev* 2001;15:3059–87.
- Thirant C, Ignacimoutou C, Lopez CK, Diop M, Le Mouel L, Thiollier C, et al. ETO2-GLIS2 hijacks transcriptional complexes to drive cellular identity and self-renewal in pediatric acute megakaryoblastic leukemia. *Cancer Cell* 2017;31:452–65.
- Masetti R, Bertuccio SN, Astolfi A, Chiarini F, Lonetti A, Indio V, et al. Hh/Gli antagonist in acute myeloid leukemia with CBFA2T3-GLIS2 fusion gene. *J Hematol Oncol* 2017;10:26.
- Aplenc R, Meshinchi S, Sung L, Alonzo TA, Pollard J, Gerbing R, et al. The addition of bortezomib to standard chemotherapy for pediatric acute myeloid leukemia has increased toxicity without therapeutic benefit: a report from the Children's Oncology Group. *Blood* 2016;128:899.
- Cooper TM, Franklin J, Gerbing RB, Alonzo TA, Hurwitz C, Raimondi SC, et al. AAML03P1, a pilot study of the safety of gemtuzumab ozogamicin in combination with chemotherapy for newly diagnosed childhood acute myeloid leukemia: a report from the Children's Oncology Group. *Cancer* 2012;118:761–9.
- Gamis AS, Alonzo TA, Meshinchi S, Sung L, Gerbing RB, Raimondi SC, et al. Gemtuzumab ozogamicin in children and adolescents with de novo acute myeloid leukemia improves event-free survival by reducing relapse risk: results from the randomized phase III Children's Oncology Group trial AAML0531. *J Clin Oncol* 2014;32:3021–32.
- Lange BJ, Smith FO, Feusner J, Barnard DR, Dinndorf P, Feig S, et al. Outcomes in CCG-2961, a children's oncology group phase 3 trial for untreated pediatric acute myeloid leukemia: a report from the children's oncology group. *Blood* 2008;111:1044–53.
- Eidenschink Brodersen L, Alonzo TA, Menssen AJ, Gerbing RB, Pardo L, Voigt AP, et al. A recurrent immunophenotype at diagnosis independently identifies high-risk pediatric acute myeloid leukemia: a report from Children's Oncology Group. *Leukemia* 2016;30:2077–80.
- Feng Y, Wang Y, Zhu Z, Li W, Sussman RT, Randall M, et al. Differential killing of CD56-expressing cells by drug-conjugated human antibodies targeting membrane-distal and membrane-proximal non-overlapping epitopes. *MAbs* 2016;8:799–810.
- Whiteman KR, Johnson HA, Mayo MF, Audette CA, Carrigan CN, LaBelle A, et al. Lorvotuzumab mertansine, a CD56-targeting antibody-drug conjugate with potent antitumor activity against small cell lung cancer in human xenograft models. *MAbs* 2014;6:556–66.
- Dull T, Zufferey R, Kelly M, Mandel RJ, Nguyen M, Trono D, et al. A third-generation lentivirus vector with a conditional packaging system. *J Virol* 1998;72:8463–71.

22. Haas BJ, Dobin A, Li B, Stransky N, Pochet N, Regev A. Accuracy assessment of fusion transcript detection via read-mapping and de novo fusion transcript assembly-based methods. *Genome Biol* 2019;20:213.
23. Robertson G, Schein J, Chiu R, Corbett R, Field M, Jackman SD, et al. De novo assembly and analysis of RNA-seq data. *Nat Methods* 2010;7:909–12.
24. Luo W, Friedman MS, Shedden K, Hankenson KD, Woolf PJ. GAGE: generally applicable gene set enrichment for pathway analysis. *BMC Bioinformatics* 2009;10:161.
25. Zhou X, Edmonson MN, Wilkinson MR, Patel A, Wu G, Liu Y, et al. Exploring genomic alteration in pediatric cancer using ProteinPaint. *Nature Genetics* 2015;48:4–6.
26. Neapolitan R, Horvath CM, Jiang X. Pan-cancer analysis of TCGA data reveals notable signaling pathways. *BMC Cancer* 2015;15:516.
27. Sever R, Brugge JS. Signal transduction in cancer. *Cold Spring Harb Perspect Med* 2015;5.
28. Binder JX, Pletscher-Frankild S, Tsafou K, Stolte C, O'Donoghue SI, Schneider R, et al. COMPARTMENTS: unification and visualization of protein subcellular localization evidence. *Database (Oxford)* 2014;2014:bau012.
29. Schroeder T. Hematopoietic stem cell heterogeneity: subtypes, not unpredictable behavior. *Cell Stem Cell* 2010;6:203–7.
30. Schepers K, Campbell TB, Passegue E. Normal and leukemic stem cell niches: insights and therapeutic opportunities. *Cell Stem Cell* 2015;16:254–67.
31. Graham DK, DeRyckere D, Davies KD, Earp HS. The TAM family: phosphatidylserine sensing receptor tyrosine kinases gone awry in cancer. *Nat Rev Cancer* 2014;14:769–85.
32. Lagadec C, Meignan S, Adriaenssens E, Foveau B, Vanhecke E, Romon R, et al. TrkA overexpression enhances growth and metastasis of breast cancer cells. *Oncogene* 2009;28:1960–70.
33. Salgia R. MET in lung cancer: biomarker selection based on scientific rationale. *Mol Cancer Ther* 2017;16:555–65.
34. Mochmann LH, Bock J, Ortiz-Tanchez J, Schlee C, Bohne A, Neumann K, et al. Genome-wide screen reveals WNT11, a non-canonical WNT gene, as a direct target of ETS transcription factor ERG. *Oncogene* 2011;30:2044–56.
35. Knoll S, Furst K, Kowtharapu B, Schmitz U, Marquardt S, Wolkenhauer O, et al. E2F1 induces miR-224/452 expression to drive EMT through TXNIP down-regulation. *EMBO Rep* 2014;15:1315–29.
36. Ling H, Pickard K, Ivan C, Isella C, Ikuo M, Mitter R, et al. The clinical and biological significance of MIR-224 expression in colorectal cancer metastasis. *Gut* 2016;65:977–89.
37. Tellez CS, Juri DE, Do K, Picchi MA, Wang T, Liu G, et al. miR-196b is epigenetically silenced during the premalignant stage of lung carcinogenesis. *Cancer Res* 2016;76:4741–51.
38. Yu PY, Lopez G, Braggio D, Koller D, Bill KLJ, Prudner BC, et al. miR-133a function in the pathogenesis of dedifferentiated liposarcoma. *Cancer Cell Int* 2018;18:89.
39. Kumar R, Raghava GPS. ApoCanD: database of human apoptotic proteins in the context of cancer. *Sci Rep* 2016;6:20797.
40. Su X, Chen D, Yang K, Zhao Q, Zhao D, Lv X, et al. The circadian clock gene PER2 plays an important role in tumor suppression through regulating tumor-associated genes in human oral squamous cell carcinoma. *Oncol Rep* 2017;38:472–80.
41. Thompson TC. Glioma pathogenesis-related protein 1: tumor-suppressor activities and therapeutic potential. *Yonsei Med J* 2010;51:479–83.
42. Lamba JK, Cao X, Raimondi SC, Rafiee R, Downing JR, Lei S, et al. Integrated epigenetic and genetic analysis identifies markers of prognostic significance in pediatric acute myeloid leukemia. *Oncotarget* 2018;9:26711–23.
43. Favreau AJ, McGlaufflin RE, Duarte CW, Sathyanarayana P. miR-199b, a novel tumor suppressor miRNA in acute myeloid leukemia with prognostic implications. *Exp Hematol Oncol* 2015;5:4.
44. Koshizuka K, Hanazawa T, Kikkawa N, Arai T, Okato A, Kurozumi A, et al. Regulation of ITGA3 by the anti-tumor miR-199 family inhibits cancer cell migration and invasion in head and neck cancer. *Cancer Sci* 2017;108:1681–92.
45. Milde T, Shmelkov SV, Jensen KK, Zlotchenko G, Petit I, Rafii S. A novel family of slitrk genes is expressed on hematopoietic stem cells and leukemias. *Leukemia* 2007;21:824–7.
46. de Rooij JD, Hollink IH, Arentsen-Peters ST, van Galen JF, Berna Beverloo H, Baruchel A, et al. NUP98/JARID1A is a novel recurrent abnormality in pediatric acute megakaryoblastic leukemia with a distinct HOX gene expression pattern. *Leukemia* 2013;27:2280–8.
47. de Rooij JD, Masetti R, van den Heuvel-Eibrink MM, Cayuela JM, Trka J, Reinhardt D, et al. Recurrent abnormalities can be used for risk group stratification in pediatric AMKL: a retrospective intergroup study. *Blood* 2016;127:3424–30.
48. Gilliland DG. Molecular genetics of human leukemias: new insights into therapy. *Semin Hematol* 2002;39(4 Suppl 3):6–11.
49. Consortium EP. An integrated encyclopedia of DNA elements in the human genome. *Nature* 2012;489:57–74.
50. Lian XY, Zhang W, Wu DH, Ma JC, Zhou JD, Zhang ZH, et al. Methylation-independent ITGA2 overexpression is associated with poor prognosis in de novo acute myeloid leukemia. *J Cell Physiol* 2018;233:9584–93.